A smart system for the automatic evaluation of green olives visual quality in the field

Rafael R. Sola-Guirado[1]*, Sergio Bayano-Tejero[1], Fernando Aragón-Rodríguez[1], Bruno Bernardi[2], Souraya Benalia[2], Sergio Castro-García[1]

[1] G.I. AGR 126 "Mecanización y Tecnología Rural". Universidad de Córdoba. Campus Rabanales, Ctra. Nacional IV, km. 396. 14014. Córdoba.

[2] Dipartimento di Agraria, Università degli Studi Mediterranea di Reggio Calabria, Località Feo di Vito snc, Reggio Calabria, 89122 (RC), Italy.

* Corresponding author: ir2sogur@uco.es
https://doi.org/10.1016/j.compag.2020.105858

Keyworks: image analysis, supervised training, maturity index, weight estimation, ~~affordable~~tool, decision making

Abstract

Monitoring some of the parameters that affect the quality of table olives for green processing is fundamental in a farmer's decision making. This work develops an affordable system for in-the-field evaluation of fruit calibre, ripeness and bruise index. The system consists of an illuminated cube that ~~takes photographs~~acquires images of fruit samples and generates an instantaneous report, using computer vision techniques implemented in software. To do this, it was necessary to determine models of fruit weight and size and also the colour regions (RGB colour space) involved in olive maturity indexes. Moreover, supervised training models were created to perform image segmentation (background and bruising areas). Error in the estimation of fruit weight was very low (R^2=0.9), and prediction of the maturity index (MI) was quite good, with an accuracy of 0.66 and 0.91 for manually sorted olives in MI0 and MI1 respectively (green processing). Prediction of MI2 had lower precision (0.48) when the fruit was changing to black-purple and the bruising spots were confused with fruit area because of determined similarities in colour. The error in the estimated bruise index was lower for MI0 (RMSE=2.42) than for MI1 (RMSE=3.78), both of which are suitable for an estimation of quality in the field. Overall, the system's performance reveals promising results for a quick, easy and accurate evaluation of the external parameters that define the quality of olives. The models obtained could be useful for other purposes.

Introduction

The world production of table olives is approximately 2.9 million metric tons per year (IOC, 2018). The Spanish style, which is one of the most popular preparation methods for olive consumption, requires green olives harvested during the ripening cycle when they have reached a determined size, but prior to colour change. Certain parameters like ripeness, size or defects define the commercial category to which olives will be assigned (FAO, 2013). These parameters therefore influence olive processing, and consequently the final product price.- Farmers control some of the parameters, which involve decision-making about fundamental growing practices such as determination of the optimal harvest time, the choice of harvesting procedure to reduce damage, or the selection of the most suitable trees to harvest. Hence, monitoring olive ripening, size and defects in the field becomes crucial so as not to compromise the final quality of table olives. Monitoring often employs destructive analyses in controlled laboratories with what can be relatively sophisticated equipment.

Colour is the principal determinant of the development stage of olive ripeness. For Spanish style processing, it is important to control the development of ripening to reach "green-ripe olives". Normally, olive colour is determined according to different classes established long ago (Ferreira, 1979) or maturity index groups (Guzman, 2015) that consider the percentage of green, yellow, purple and black colour on the fruit. However, there is a lack of values to determine the proper colour for sorting, which is in fact often performed visually by experienced operators in the filed or in the processing units. However, this method presents drawbacks. Some authors have designed algorithms to predict olive class or maturity index (MI) based on colour channels (Diaz 2000; Furferi, 2010; Dumanay 2016) with promising results.

In addition, the size of olives is determined in industry considering the number of fruits contained in one kilogram, and this operation is usually performed using mechanical screening or sorting machines based on image analysis. The estimation of fruit weight by determining its geometry using image analysis has given good results for citrus fruit (Omid, Khojastehnazhand, & Tabatabaeefar, 2010) and olives (Ponce, Aquino, Millán, & Andújar, 2018). The application of weight-size regressions could even be carried out automatically by techniques that predict the variety of olive samples (Martinez et al, 2018).

Defects in table olives affect their commercial value (Riquelme et al., 2008) and can mean that some olives may be discarded for green processing. Other than biotic agents or unfavourable climatic conditions, defects may also occur during the manual or mechanical harvesting process, causing spots that undergo an oxidation process and generate browning in the impacted zone (bruising). The level of damage can be estimated by the ratio of bruised area to total fruit area (bruise index) (Jiménez-Jiménez et al., 2013). Determination of bruised area is a difficult task to perform automatically with traditional image analysis techniques. This is due to both the complexity of spot shapes and their colour, which that can be confused with that of certain stages of olive ripeness. Machine learning techniques may be applied to extract some olive parameters or grading with good results (Dıaz et al., 2004) and could also be used in industrial applications *(*Jodar Lazaro et al., 2020*).*

There are several studies and reviews that have researched the technologies available for assessing fruit and vegetable quality (Arendse et al., 2018; Bhargava & Bansal 2018; Ortaç- et al., 2016; Srivastava et al., 2018; Tsouvaltzis et al., 2020; Zhang et al., 2018), but also for olive quality (Navarro-Soto et al., 2018) and specifically for table olives (Campus et al., 2018). In recent years, the industry has implemented all these advances in automated fruit inspection using powerful commercial equipment (Cayuela 2010; Serranti, 2018) specifically designed for product analysis according to the criteria of the target market. However, the evaluation of fruit in the field is still a challenge, although new developments have arisen that are able to perform the estimation of certain fruit parameters from terrestrial mobile platforms (Kohno et al., 2011; Cubero et al., 2014) or from drones (Méndez et al., 2019; Apolo-Apolo et al., 2020).

Considering the above, our work investigates the feasibility of a device based on a computer vision system for the automatic evaluation in the field of external parameters such as ripening, size and bruises. Such a device will be a ready-to-use tool for farmers or technicians that would avoid the need for expensive instruments or low-accuracy manual procedures. For ripening assessment in particular, the proposed method aims to identify a threshold colour for each maturity class and sort the analysed olives according to class. In addition, the study proposes shape recognition based on particle analysis to determine the main diameters of the fruit (fitted ellipse), and the estimation of its weight and calibre by applying a previously determined model. Regarding bruises, this work aims to determine the bruised area and bruise index of fruits by applying different training models according to their previously determined maturity class. Overall, this work aims to develop a portable, affordable system for the automatic evaluation of green table olive quality in the field, assess its suitability, and generate the necessary models required to achieve this purpose.

Materials and Methods

Development of the system for the evaluation of olive parameters

A system for the automatic evaluation of olive quality of (SAEOQ) has been developed (Figure 1). It is a portable device of 0.8 x 0.8 x 0.8 m, and weighs 5 kg, which allows the image acquisition of fruit samples ~~photographs to be taken~~ in the field. The box consists of a tubular PVC chassis covered with a reflective plastic fabric that blocks out external lighting conditions. Inside the box there is a housing for blue foam, 0.18 m square trays that have perforations to hold 20 olive samples. Under the housing, covered by the diffuser screen, 4 LED bars of 5500ºK ((HPB-60xd) are positioned at an orientation of 30º to the horizontal plane. These bars emit a constant level of illumination of 13.95±0.57 lux in the area of the tray. There is a support 0.85 m above the tray to place a conventional digital camera. This work used an AD-130 GE DE (JAI) camera with a low resolution of 1.3Mpx, however, any low-cost camera could be employed. The camera was synchronized using an Arduino Nano system and SSR relays with lighting (0.3 s exposure) via a trigger button. The images were automatically acquired from a laptop (IdeaPad Z510, Lenovo, China) that runs a specific software designed for the acquisition and automatic analysis of the images.

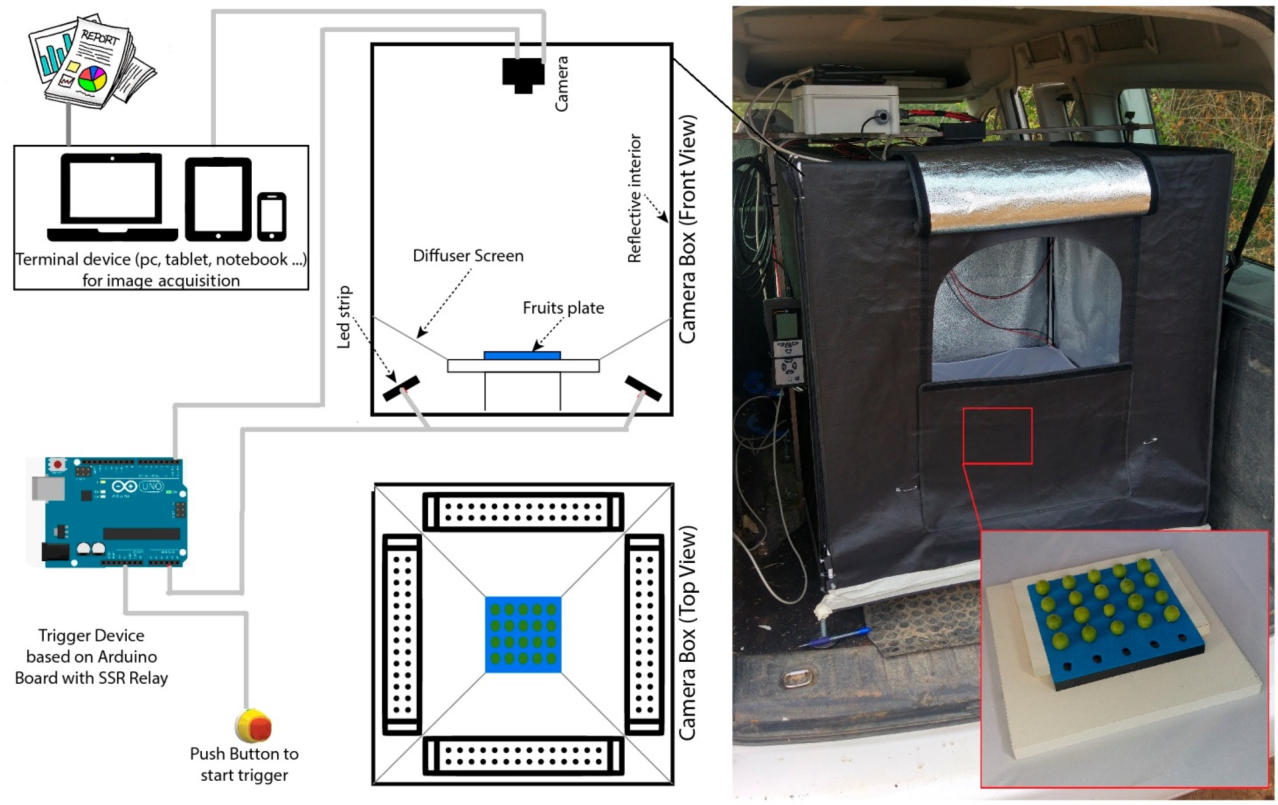

Figure 1. Device (SAEOQ) developed for automatic image acquisition and analysis

Development of the software for image analysis

We designed and implemented software in the terminal device connected to (SAEOQ) to analyse the images. Several field tests were conducted to programme the software. First, it was necessary to determine the models to implement in the software, and then validate the system. The final configuration of the software's main stages was determined from the experimental test results, and the description of these steps follows. Figure 2 shows some examples of the outputs that the algorithm would report after each stage.

A) <u>Image acquisition</u>: The camera captures the image, which is loaded by the software.
B) <u>Image processing</u>: A Gaussian Smoothing filter (window: 5 px, sigma: 1) is applied to create a slight defocusing that smooths the image without losing detail and removes possible noise (Haff et al., 2013). Subsequent application of the Kuwahara filter (windows 9 px, sigma: 1) allows removal of gradients and highlights the edges without the loss of important information (Djurovic, 2017). Finally, an HSL (Hue, Saturation, Lightness) adjustment is performed to reduce possible shadows on the fruits and adjust the lighting of the image to that of the colorimeter used (6500 K) for later comparison.

C) Fruit segmentation: A Random Forest algorithm (Breiman, 2001) is applied. This is based on loading a supervised learning model (TM_Fruit) trained to remove the background. The remaining pixels are then identified as belonging to the fruit.

D) Calculation of fruit size and calibre: Each fruit image is cropped and fitted to a rectangle that circumscribes the shape of the fruit. A calibration factor (pixels per mm) is then applied. The dimensions of the rectangle are considered as fruit diameter (width) and fruit length (height) (mm). Fruit area (mm^2) is the conversion of the total number of pixels by their distance. A mathematical formula obtained from field tests (data shown in results section) is then applied to estimate fruit weight fruit according to fruit size, and therefore to estimate its calibre. If the fruit belongs to the calibre class that contains more than 420 fruit in a kilogram (small calibre), it is labelled with the category of disposable fruit, as industry would discard this calibre.

E) Calculation of Colour: The colour of each pixel in the red, green and blue channels (RGB.R, RGB.G, RGB.B) is calculated.

F) Calculation of Maturity Index (MI): Each fruit pixel is assigned to a colour group according to the thresholds calculated previously from field test results (data shown in results section). Any pixel outside these thresholds was identified as undefined and was not considered for the calculation. The fruit is then categorised into a maturity index group (Equation 1) following one of the most common sorting systems in industry (Guzman, 2015):

$$f(x) \equiv \begin{cases} MI0,\ if\ \left(\sum_{dg=1}^{n} x_{dg} > \sum_{yg=1}^{n} x_{yg}\right) \&\& \left(\sum_{rp=1}^{n} x_{rp} = 0\right) \&\& \left(\sum_{b=1}^{n} x_{b} = 0\right) \\ MI1,\ if\ \left(\sum_{dg=1}^{n} x_{dg} < \sum_{yg=1}^{n} x_{yg}\right) \&\& \left(\sum_{rp=1}^{n} x_{rp} = 0\right) \&\& \left(\sum_{b=1}^{n} x_{b} = 0\right) \\ MI2,\ if\ \left(\sum_{dg=1}^{n} x_{dg} + \sum_{yg=1}^{n} x_{yg}\right) > \left(\sum_{rp=1}^{n} x_{rp} + \sum_{b=1}^{n} x_{b}\right) \\ MI3,\ if\ \left(\sum_{dg=1}^{n} x_{dg} + \sum_{yg=1}^{n} x_{yg}\right) < \left(\sum_{rp=1}^{n} x_{rp} + \sum_{b=1}^{n} x_{b}\right) \\ MI4,\ if\ \left(\sum_{b=1}^{n} x_{b} > \sum_{rp=1}^{n} x_{rp}\right) \&\& \left(\sum_{dg=1}^{n} x_{dg} = 0\right) \&\& \left(\sum_{yg=1}^{n} x_{yg} = 0\right) \end{cases} \quad \text{Eq. 1}$$

~~a. MI0: Sum of deep green pixels > Sum of yellow-green pixels and without purple or black pixels.~~

~~b. MI1: Sum of deep green pixels < Sum of yellow-green pixels and without purple or black pixels.~~

~~c. MI2: Sum of yellow-green pixels > Sum of purple or black pixels.~~

~~d. MI3: Sum of yellow-green pixels < Sum of purple or black pixels.~~

~~e. MI4 or higher: Majority of black pixels and without deep green and yellow-green.~~

where x: pixel; dp: deep green; yg: yellow-green; rp: red/purple; b: black

G) Bruising segmentation: A Random Forest algorithm is applied. It loads different supervised learning models, depending on whether their index is MI0 or MI1 (TM_BrIM0, TM_BrMI1), which have been previously trained to determine the bruising area of the fruit. Fruit with MI1 have areas with changing colour that can be confused with bruising, but this does not occur in fruit with MI0. Fruit with MI2 or higher are not analysed because they would not be considered for green olive processing

H) Calculation of Bruising Index (BI): The bruising index (%) is calculated based on the relation between bruise area and fruit area. The application then classifies the fruit into different categories of damage (zero, slight, moderate, severe, mutilated) depending on the bruise index (Jiménez-Jiménez et al., 2013).

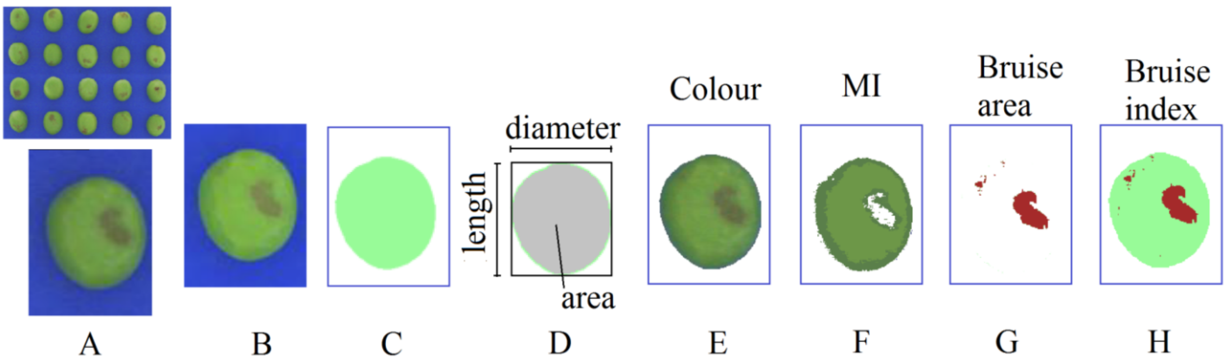

Figure 2. Main steps of the algorithm designed for olive quality assessment

All of the previously described steps are carried out thanks to an application that was developed in '.NET' language for Windows and which allows importing an image file, applying filters, loading the created training models and performing an analysis of each image to extract the main external quality parameters of the fruit (Figure 3). Several reusable libraries have been programmed for the app so that it is adaptable to different needs. The app runs whatever the machine learning algorithm used for the training and filters or for other configurations. All the cyclic processes have been programmed using multithreaded programming so that it is possible to use all processor cores, and the process can be accelerated. The application allows loading of as many images as the user wishes, and adds the results of each fruit as well as their averages to the report before exporting them to other files.

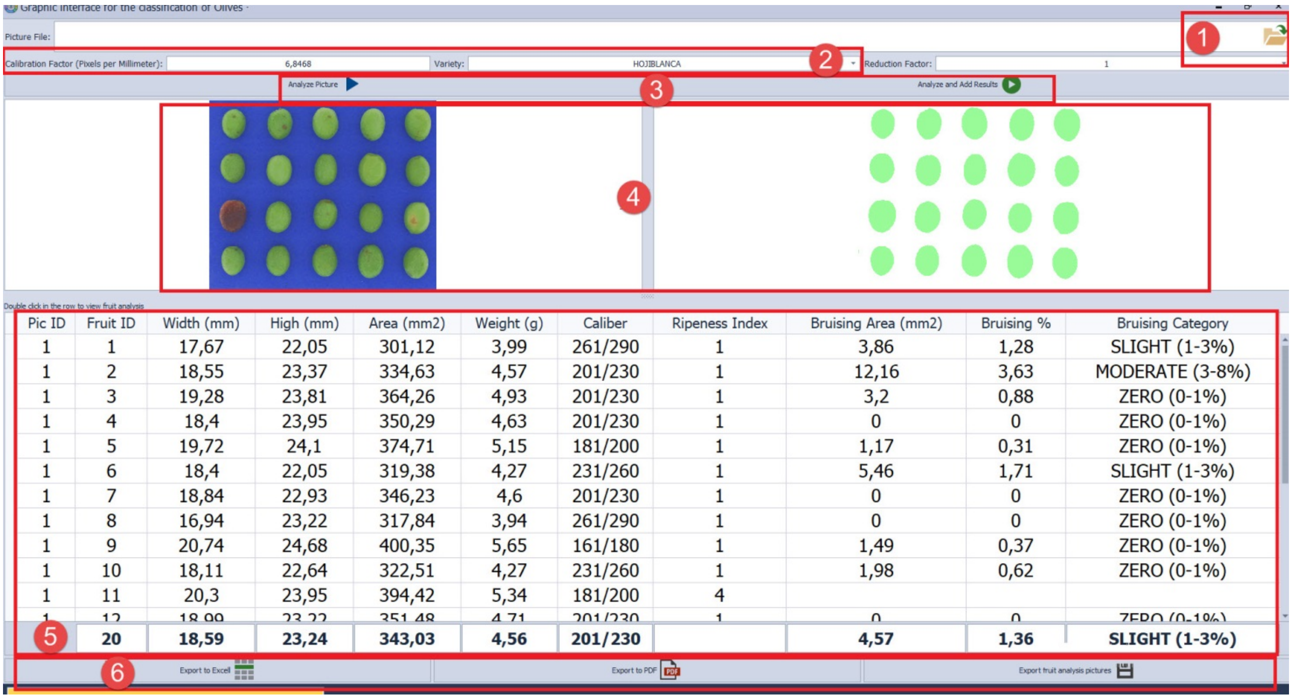

Figure 3. Interface developed for the automatic evaluation of external parameters of table olives using SAEOQ. 1: Button for loading image; 2: Calibration factor (pixels per millimetre) and selection of olive variety; 3: Buttons for analysing the image and deleting the previously analysed data or adding the data to those previously analysed; 4; Original and segmented image; 5: Data analysed; 6: Buttons for exporting the data analysed (.xls file, .pdf file) and segmented images (.tiff file)

Field test carried out for programming the software.

Field tests were carried out on two different plots in the south of Spain, Almodóvar del Río (37.855472, -4.993882) planted with the Manzanilla variety, and Aguilar de la Frontera (37.457139,-4.805250) planted with the Hojiblanca variety. These are two common table olive varieties in the green processing industry. Six trials were conducted on each plot on a weekly basis from 19th September to 24th October 2019 (the season for table olive harvesting). During each trial, fruit were detached manually and mechanically using a shaker comb and a branch shaker. Random samples were taken of 760 Hojiblanca and 840 Manzanilla fruits, which had a normal distribution of maximum and minimum diameters and weights (Kolmogorov-Smirnov, $p > 0.05$). One hundred and fifty minutes after harvesting, the time during which the devolution of fruit bruising stabilizes (Jiménez-Jiménez et al., 2013), the fruit samples were placed on a tray (20 samples per tray) to take pictures with SAEOQ.

The data were divided into two 50/50 datasets, one dataset for training and validation and one for testing. The training and validation dataset served to train and select the models using k-5 cross validation whereas the testing dataset was used to evaluate the estimations calculated for the software. To this end, the samples were manually measured to obtain the parameters shown in Figure 3 as follows.

- Fruit length and fruit diameter: measured manually with a digital Vernier calliper (Pittsburgh 61585, USA).
- Fruit weight (w): obtained with a precision scale (Gram SPX6000).
- Colour (CIE*Lab*): determined using a colorimeter (Konica Minolta CR-400, China) as the average of two readings on different zones of the fruit. The bruising area of some of the most damaged fruit was also measured.
- Maturity index (MI): according to the classes studied by Guzman (2015), with an experienced, trained operator classifying the samples visually.
- Fruit area and bruise area: digitally determined from the pictures taken with SAEOQ by an expert, who manually marked areas (px^2) of interest and scaled them using Ilastik (General Public License, Heidelberg, Germany) software.
- Bruise index (BI), calculated as the percentage of the area of fruit that was bruised. Calculations did not include spots less than 1 mm^2.

Some of the following measurements were used to determine the models implemented in the software.

1) Determination of the models implemented in the software.

1.1. Training models

We obtained different training models to run the described software. An expert used the software to manually train image segmentation by selecting the pixel that corresponded to each class employed in each model (background, fruit, bruising). A data map of the selected pixel was then imported from the application to generate the models. The first model (TM_Fruit) was used to segment the background and the fruit in the image, as well as to determine its geometry. The same number of pixels was selected for the "background" class and for the "fruit" class (approximately 3000 each) so that there was a balance of classes. The second and third model (TM_BrIM0, TM_BrMI1) were used to determine how much fruit was bruised. We classified fruit images visually according to different maturity indexes, selecting at least 2000 pixels for the "bruise" class and for the "fruit" class, although the balancing of classes was not so high because the "fruit" class was predominant among fruit with zero damage.

A Random Forest algorithm and a Naive Bayes algorithm were used as learning methods for constructing the models. As its hyperparameter, Random Forest used 200 decision trees to estimate predictions, whereas Naive Bayes employed the Gaussian classifier. The pictures acquired by SAEOQ in the field tests provided the images for training. The original images and those processed with the previously described filters were analysed with both algorithms to choose the most proper configuration with the least prediction error.

1.2. Weight and maturity index estimation.

Stage D (Figure 2) of the software reports a fruit calibre estimation based on fruit weight estimation. We obtained weight estimation by associating the olive weights recorded in the field with the fruit length and diameter calculated from the segmented picture. Then, a correlation was determined from the 1600 fruit samples. Differences between the two varieties studied were considered in order to properly implement the correlation obtained in the software.

Stage E (Figure 2) calculates the fruit maturity index according to the colour thresholds (deep green, yellow-green, purple and black) of their pixels. To determine these colour thresholds, an expert selected the zones where these colours appeared on approximately 200 randomly chosen olives during the test. As RGB colour space is device dependent (Menesatti et al., 2012), these colour zones were also measured with the colorimeter for calibration purposes. The colour values were transformed to RGB space (the colour space used by the software). Only the Green and Red channels were used as they are the most suitable for olive segmentation (Gatica et al., 2013). Some regions were determined according to their location on the R-G chart taking into account no overlaps so as to avoid conflict in the classification software (stage E).

2) Assessment of SAEOQ.

2.1 Device performance evaluation

Four image templates (Figure 4) were made with several known shapes that simulate configurations of different fruit sizes and bruising. The digital images were treated with different resolutions of 72, 150 and 300 dpi, and the software automatically calculated the BI to evaluate error obtained due to the algorithm itself. These images were then printed on matte canvas and placed on the flat trays for digital image acquisition with SAEOQ, in order to evaluate the error due to environmental conditions. For this last step, we installed a digital camera with a 10.2 Mpx resolution (Nikon Corporation, D80, Tokyo, Japan) on

SAEOQ and set it at a speed of ISO-100, with an f/9 aperture, an exposure time of 1/125 s, and a focal distance of 35 mm, with no flash. The intention was to determine the feasibility of using a low resolution with a low-cost camera.

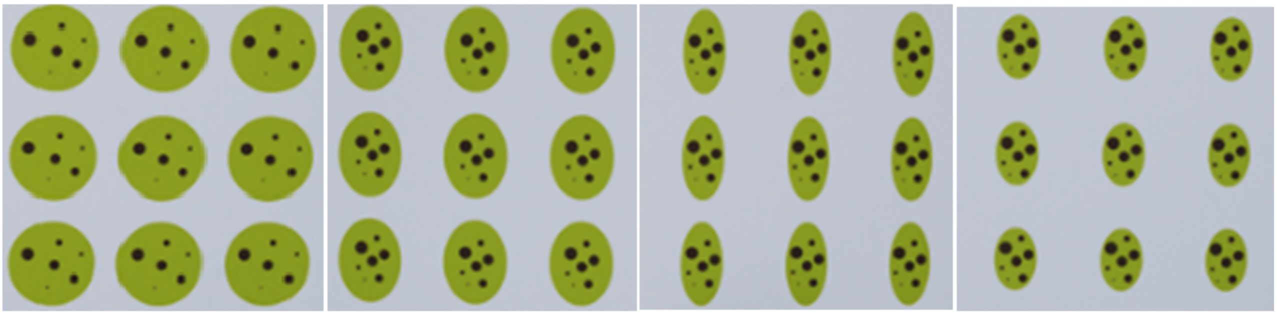

Figure 4. Ellipses used for the calibration setting of SAEOQ: (40x40 mm), (30x40 mm), (20x40 mm), (20x30 mm) with circular spots of 1-6 mm²

We connected different hardware systems to SAEOQ to evaluate the system velocity for analysing the images obtained by the camera (JAI) with real fruit, with the aim of determining the feasibility of using affordable hardware in the field.

2.2 Evaluation of external parameter prediction.

The manually recorded parameters and those obtained automatically with the software from 50% of the fruit images used for the training tests were compared in order to study the feasibility of this system for the automatic analysis of table olive quality in the field.

Results and discussion

1) Determination of the models implemented in the software.

1.1. Training models

The application of adaptive or global threshold techniques reported inaccuracy results for brusing segmentarion (data not shown) making necessary the use of machine learning algorithms. The configuration of the Gaussian-Kuwahara-HSL filters was determined with successive tests until the configuration that gave the highest resolution in the definition of edges, homogenization of colours and highlighting of bruising was obtained. Table 1 shows the difference in errors obtained before and after applying filters on the raw image captured from SAEOQ, and also between the algorithms used for the creation of the applied models (Naive Bayes and Random Forest), by means of a cross validation using 20% of the image data in the training models.

*Table 1. Mean absolute percentage error (%) of cross validation of the training models for determining the fruit (TM_Fruit) and the bruising with MI0 (TM_BrMI0) or MI1 (TM_BrMI0) from original and processed images. Cells marked with * show the error of the selected configuration for the software used.*

Algorithm	Classes	TM_Fruit by images		TM_BrMI0 by images		TM_BrMI1 by images	
		original	processed	original	processed	original	processed
Naive Bayes	Background	0.0	0.0	0.0	0.0	0.07	0.0
	Fruit	0.35	0.0	29.63	26.71	31.55	29.62
	Bruise	-	-	14.08	7.13	8.34	8.09
Random Forest	Background	0.0	0.0*	0.0	0.0*	0.0	0.0*
	Fruit	0.0	0.0*	4.47	1.56*	5.33	2.48*
	Bruise	-	-	10.37	6.43*	14.50	6.52*

The results indicate that the configuration with the least error at a global level is processed images using the Random Forest algorithm, so this was implemented in the software described in the materials and methods section. Fruit-background segmentation was performed out in a very precise manner in all of the possible configurations. For bruising segmentation in MI0 or MI1, there was not a large difference in the use of filters with Naive Bayes. Accuracy improves approximately 21% with the use of Random Forest, reducing error by almost half in both the fruit and bruise class with the use of filter settings, as noted by Kumar Dash and

Panda (2016). It is highly advisable to produce the least possible error with the TM_Br models to predict the pixel that belongs to the bruise class. However, the error obtained in the sorting (Table 2), which was around 7%, could provide low accuracy predictions when estimating real bruising on fruit.

1.2.1 Weight and maturity index estimation.

There were significant differences in fruit diameter, length and weight between Manzanilla and Hojiblanca varieties (T-student test, $p < 0.05$). This suggests that the software should include the variety to predict fruit weight (Figure 3, number 2). Therefore, multiple linear regressions were obtained between the fruit weight and the fruit diameter and length for Manzanilla ($R^2 = 0.90$, Equation 1) and for Hojiblanca ($R^2 = 0.91$, Equation 2) (Figure 5). The high adjustment of the linear correlations obtained ensures a good estimation of fruit calibre within the tolerance that regulations allow.

$$\text{Estimated weight (g)} = -7.175 + 0.225 * \text{Fruit length (mm)} + 0.352 * \text{Fruit diameter (mm)} \qquad \text{Equation 1}$$

$$\text{Estimated weight (g)} = -6.780 + 0.171 * \text{Fruit length (mm)} + 0.397 * \text{Fruit diameter (mm)} \qquad \text{Equation 2}$$

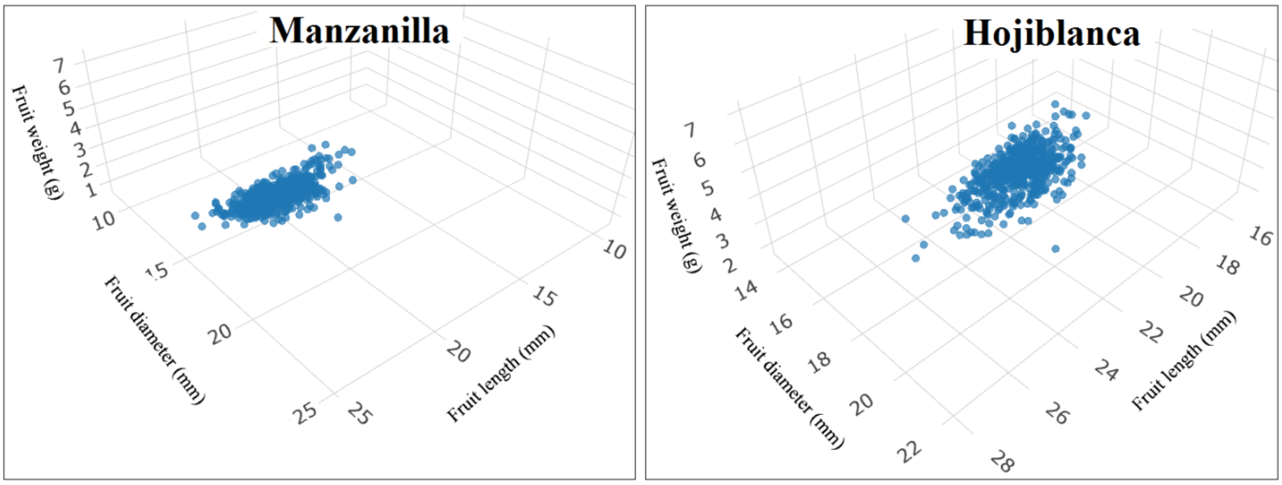

Figure 5. Correlation obtained to estimate fruit weight based on fruit diameter and fruit length

1.2.2 Maturity index estimation

Figure 6 represents the RGB.R and RGB.G colour values measured on different fruit zones, and their classification into groups. It is possible to sort and delimit these groups by defined regions so as to avoid overlaps between them and fit them around the majority of the represented points (Table 2). The results obtained must be taken with great caution because even if the equipment were the same as that employed for this paper, the values or regions might vary depending on different lighting conditions when using the CIE*Lab* scale.

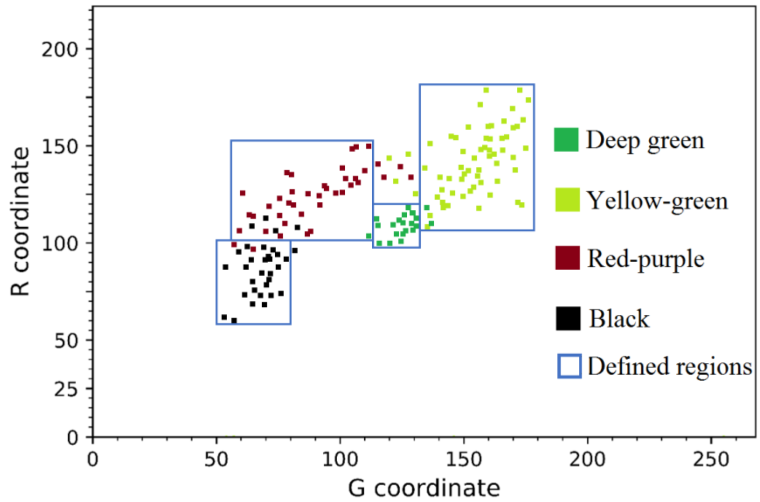

Figure 6. Colours measured (RGB.R and RGB.G) in areas of the fruit and defined regions that fit the majority of the same group points

Table 2. RGB.R and RGB.G values of the defined regions of colours obtained for the maturity index sorting

Colour	R min.	R max.	G min.	G max.
Deep green	97	120	118	135
Green-yellow	105	182	136	182
Red-purple	103	157	58	117
Black	55	102	52	86

2) Assessment of SAEOQ.

1.1 Performance of the device

Table 3 shows the relative error between the bruise index estimated with the software and calculated theoretically with the known fruit-spot geometry from the image templates (Figure 5). The results are compared according to the different resolutions without any substantial differences between the resolutions of 150 dpi and 300 dpi. Thus, the average resolution seems to be acceptable for the application presented in this paper because the mean resolution of the images acquired in the field tests with the JAI camera was 173 dpi. Moreover, the use of a higher resolution would involve a higher processing speed for the software and more powerful hardware.

The error of 0.4 % due to the algorithm increases to 3.1 % when the template images are used, due to the effect of operating conditions such as lighting, camera lens, fruit location, etc. on the images . This suggests that to reduce the error, improvements could be made in environmental conditions, such as the homogeneity of lighting. Moreover, as other authors have indicated (Tu, 2009), lighting conditions influence colour perception and this factor must also be considered, which makes it necessary to correct the regions obtained with this method (Figure 7). Other possible corrective measures consist of enhancing the flatness of the camera lens, although this would prove difficult for a low-cost application. The shadows produced between the tray and fruit produce a degraded colour around the fruit perimeter that it is also possible to correct, although this implies creating adaptive holes, which is technically difficult to implement.

Table 3. Relative error of the bruise index between the theoretical calculation from known shapes (fruits and spots) and that calculated by the software from original images and from template photos.

Digital images	Resolution (dpi)	Fruit sizes in templates (diameter x length) (mm)				
		20x30	20x40	30x40	40x40	Average
originals	72	2.8 %	2.7 %	2.7 %	2.4 %	2.7 %
	150	0.5 %	0.5 %	0.5 %	0.2 %	0.4 %
	300	0.1 %	0.1 %	0.1 %	0.2 %	0.1 %
from templates photos	150	3.4 %	3.0 %	3.7 %	2.7 %	3.2%
	300	3.0 %	2.9 %	3.9 %	2.4 %	3.1 %

Table 4 shows the average time that several hardware configurations employed to analyse the images taken from *SAEOQ* in the field test, reporting results of less than a half minute for each 20 sample fruits when using a low-cost system such as hardware D.

Table 4. Average time employed by some hardware configurations to analyse the images (n= 10) acquired from SAEOQ

Hardware configuration	**A**	**B**	**C**	**D**
Processor:	Intel Core I9-9900K 3.60 Ghz	Intel Core I7-7700 HQ 2.80 Ghz	Intel Pentium G645 2.90 Ghz	AMD A6-6400K APU 3.90 Ghz
Cores	8	4	2	1
Logical processor	16	8	4	2
RAM:	32 Gb – 2666Mhz DDR4	16 Gb – 2400 Mhz DDR4	8 Gb – 1600 Mhz DDR3	12 Gb – 1600Mhz DDR3
Average time	**4.0 s**	**8.4 s**	**12.0 s**	**27.4 s**

1.3 Evaluation of the estimated parameters.

Table 5 shows the errors generated by the device in estimating geometrical parameters. The estimation of weight by fruit diameter and length is very precise and requires distinction between varieties (Ponce et al., 2018).

Table 5. MAE (Mean Absolute Error), RMSE (Root Mean Square Error) and R squared determined between the olive size and weight values calculated by the software and with manual measurement

Variety	**Parameter**	**R squared**	**MAE**	**RMSE**
Manzanilla	Diameter	0.82	0.43 (mm)	0.69 (mm)
Hojiblanca	Diameter	0.84	0.39 (mm)	0.61 (mm)
Manzanilla	Length	0.91	0.41 (mm)	0.55 (mm)
Hojiblanca	Length	0.81	0.54 (mm)	0.91 (mm)
Manzanilla	Weight	0.91	0.23 (g)	0.32 (g)
Hojiblanca	Weight	0.89	0.20 (g)	0.30 (g)

Table 6 sets out the statistical parameters calculated for the prediction of the tested fruit's maturity index. The precision indicates that the quality of the model is quite good in predicting MI1, but relatively poor for MI0. This may be a problem given that such a limitation can affect bruising estimation when it comes to applying the different models. In MI0 only one third of the real fruit that belonged in the category was identified, whereas in MI4 almost all the fruit predictions belonged to the category the expert had specified. On combining precision and recall, we obtain more balanced values for the different categories. It should be taken into account that although the estimation seems to have good accuracy, we should not consider this parameter because there is an imbalance with a greater number of samples in MI1 than in MI0.

Table 6.Statistical parameters calculated to predict the maturity index according to the percentage of fruit pixels of each defined colour group.

Maturity Index	**Precision**	**Recall**	**F1 score**	**Accuracy**	**Specificity**
MI0	0.16	0.34	0.21	0.66	0.99
MI1	0.97	0.98	0.97	0.91	0.85
MI2	0.48	0.47	0.47	0.72	0.97
MI3	0.93	0.40	0.56	0.69	0.99
MI4	0.65	0.99	0.78	0.98	0.97

It is worth mentioning that the data from the classification made by the expert is taken as real. However, the habitual criteria for sorting is highly subjective as it takes into account both colour and percentage of colour on a fruit, and we must stress the difficulty of ensuring the true accuracy of the algorithm without a criterion that establishes more quantitative data. Figure 7 shows the location of the colour in RGB.R and RGB.G coordinates of the fruit measured with the colorimeter. Ripening tendency can be appreciated with an evolution of colour that goes from left to right and from bottom to top in the transition from MI0 to MI1, and similarly, from right to left and from top to bottom in the transition from MI1 to MI4. This evolution is quite coherent with the colour threshold obtained in this work (Figure 6), suggesting the ability of computer vision-based systems to substitute conventional methods of colour evaluation, even if different maturity index groups overlap (Figure 7) making it difficult to automize the classification criterion used with extremely high accuracy.

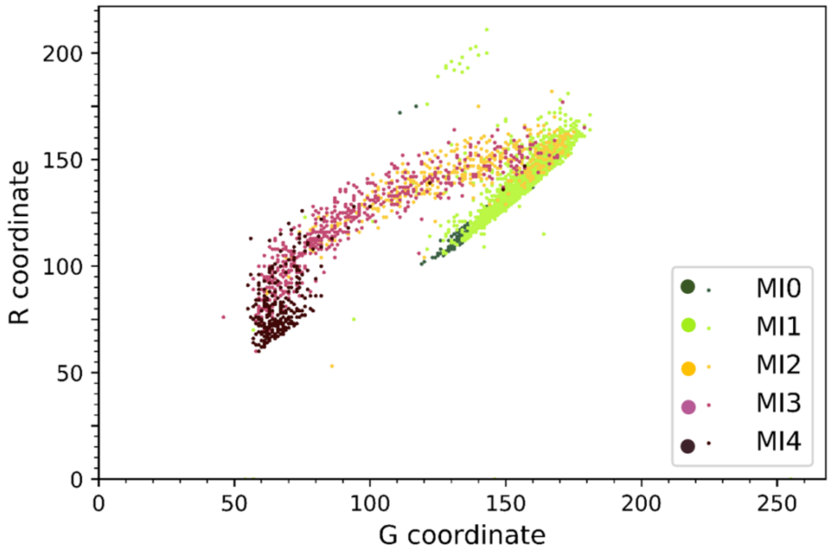

Figure 7. Location of fruit colour measurements (two per fruit) in red-green channels with the colorimeter and their manual sorting into the maturity index groups

The values of the RGB.B blue coordinate measured were very constant during the development of ripeness and had very low dispersion with values of 68.4±7.0, 77.3±7.9, 84.6±8.9, 78.1± 9.4, 68.5±5.83 for MI0, MI1, MI2, M3, and MI4, respectively. This relates with the findings of Gatica et al. (2013) and is the reason why a blue background, as used in this work, was beneficial for fruit segmentation, achieving very high results (Table 1).

The gap obtained in the RGB.G coordinate between the yellow-green and red-purple colour regions (Figure 6) was important to distinguish between MI2 and MI3 because the difference between these maturity categories is simply the percentage of pixels of each colour. Figure 8, where the categories completely overlap, illustrates this. Moreover, MI2 also overlaps with MI1, which means it is very complicated to make the distinction without using a percentage of colour pixel estimation. This implies that many pixels are not categorized in each colour region, and are not therefore considered when determining MI. However, this is decisive to avoid error when estimating the maturity group. Similarly, we observed that MI0 and MI1 fruits seem to overlap in the RGB.R - RGB.G coordinate, so only the percentage of pixels of each colour region needs to be considered.

The error generated in determining the bruise index differs widely, depending on whether the olives are classified by the algorithm as MI0 (MAE=1.44, RMSE=2.42), or MI1 (MAE=1.96, RMSE=3.78). The mean error obtained in an analysis of 90% of the fruit was approximately 5.6 % but this error significantly increased when the remaining 10% of fruit, with the highest bruise index, were introduced in the analysis, probably because these pixels are incorrectly classified as bruising. This final low precision in the bruising estimation, mainly for MI1, is due to several errors that are carried over from earlier phases in the calculation, such as lighting, MI sorting, etc. First, correctly assigning the maturity index to fruit is decisive when applying the different models and this, in turn, is conditioned by the colour calculation and by the filters used. Secondly, a large number of pixels, most of which correspond to ripening development in MI2 and MI3, are wrongly calculated as bruising due to their similarity in colour with ripe regions (Figure 8).

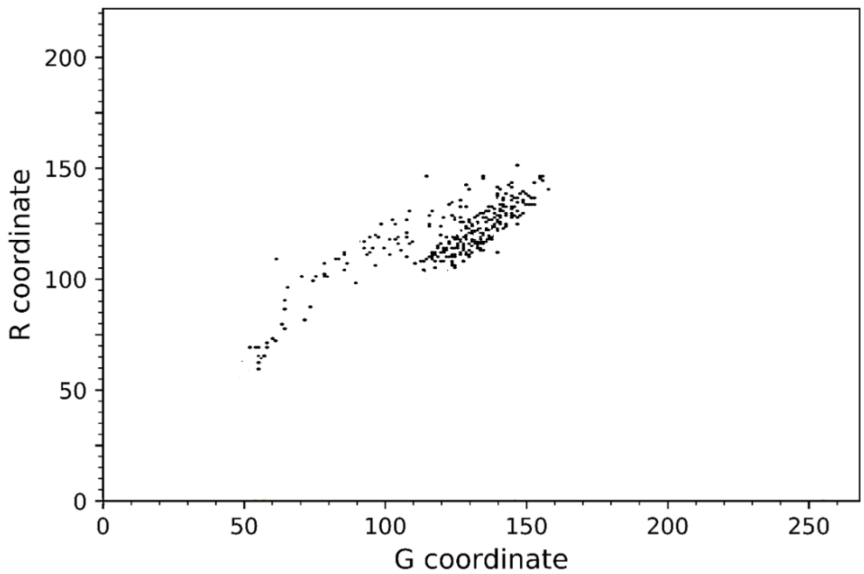

Figure 8. Location of the bruising colour measurements in the red-green channels

In general, the system developed allows the estimation of interesting global parameters for determining the quality of fruit (Opara and Pathare, 2014). It reports good performance and has an intelligent black box that determines these parameters without the need for more complex and sophisticated evaluation procedures. The tool can be used for a variety of purposes, such as agronomic decision-making in the field (Li et al., 2018) or the evaluation of harvest or post-harvest systems (Morales-Sillero et al., 2014: Sola-Guirado et al., 2020). Multi-objective evolutionary optimization techniques would enhance the algorithm obtained to produce a higher accuracy tool which would provide farmers and agricultural technicians with software tools to help them make the right decision (Chavez et al., 2019).

Conclusions

The developed system was manufactured with simple, inexpensive materials using a low-resolution camera and regular hardware, which make it an affordable system for any farmer. The device is portable and easy to use, capable of being transported in a vehicle and powered by the vehicle's battery. The software designed for the application has a simple interface that allows the automatic analysis of sample fruit images taken in the field at any moment. All of these elements mean that is an affordable system for farmers or researchers in comparison with other sophisticated, complicated industrial equipment because processing allows analysis of as many samples as the user wishes and the system provides a valuable report for other research purposes or for decision making.

The system allows fruit size, weight and calibre to be obtained with high accuracy. Although the system was studied with two varieties, it could incorporate other size-weight correlations for other varieties. The estimation of this parameter would be of value to control fruit growth and consequently to adjust agronomic actions such as fertigation. Farmers could also calculate the market value of their production.

Estimation of calibre may be of interest if combined with maturity index estimation. The proposed application provides reports that are accurate enough to determine the optimum harvest time for green olives, or even for olives destined for oil production. The colour calculation of each fruit pixel makes the application flexible for the estimation of maturity based on other criteria such as colour average. In fact, the estimation made with the criterion used in this work presents serious problems because it requires previous adjustments of the colours and subsequent calculation of their percentage. The results demonstrate that there was overlapping in colour values within the same maturity categories. Nonetheless, the rapid estimation of fruit maturity that this system provides could be valuable to control the progression of crop readiness on a farm and adequately prepare the means necessary for harvesting.

It was only possible to estimate the bruise index with a medium level of precision, and our work showed that the bruise spot can be difficult to segment, principally due to the similarities between its colour and that of the ripe regions of fruit belonging to groups MI1 and MI2. For this reason, the two training methods obtained were valuable to reduce errors in less ripe fruit. The errors obtained could be better enhanced in the earlier sorting phases, in addition to modifying some device conditions such as the trays or the lighting. Nonetheless, it is still challenging to achieve high accuracy results by employing techniques that use the visible spectrum. Fast bruise index estimation is extremely useful and difficult to estimate manually, so this method offers a great advantage in this regard. Valuable information could be extracted from these results such as the assessment of the damage caused by different harvesting systems or the evaluation of fruit defects in trees caused by meteorological phenomena.

In general, the "all in one" system developed allows a quick, easy, accurate evaluation of the main external parameters that define the quality of olives for green processing. The method used for developing the final configuration of the device can be improved by updating new training models or incorporating new models that allow adaptation for a wider range of varieties, or even adaptation of the procedures for other crops. The tools provide valuable information with a great potential for use by farmers, researchers or insurance agents.

Acknowledgements

We are very thankful for the financial support provided by the Spanish Ministry of Economy and Competitiveness (Precommercial public procurement Innolivar), co-funded by European FEDER funds, and the financial support provided by the Interprofessional Organization of Table Olive and Olive Oil, Spain https://interaceituna.com/. We would also like to thank Juan Pérez-Moya for the support given in the design of the algorithms. Finally, the RRSG thanks the help received from the Own Research Plan of University of Cordoba for conducting some trials. In addition, some instruments used in this research were funded within the framework of the National Operative Project PON Ricerca e Competitività 2007-2013, PON03PE_00090_2 "Modelli sostenibili e nuove tecnologie per la valorizzazione delle olive e dell'olio extravergine di oliva prodotto in Calabria": C38C14000060005, funded by the Italian Ministry of Education, University and Research.

References

Apolo-Apolo, O.E., Martínez-Guanter, J., Egea, G., Raja, P., Pérez-Ruiz, M., 2020. Deep learning techniques for estimation of the yield and size of citrus fruits using a UAV. Eur. J. Agron. 115, 126030. https://doi.org/10.1016/j.eja.2020.126030

Arendse, E., Fawole, O.A., Magwaza, L.S., Opara, U.L., 2018. Non-destructive prediction of internal and external quality attributes of fruit with thick rind: A review. J. Food Eng. 217, 11–23. https://doi.org/10.1016/j.jfoodeng.2017.08.009

Bhargava, A., Bansal, A., 2018. Fruits and vegetables quality evaluation using computer vision: A review. J. King Saud Univ. - Comput. Inf. Sci. https://doi.org/10.1016/j.jksuci.2018.06.002

Breiman, L. (2001). Random Forests. Machine Learning, 45 (1), 5–32. doi:10.1023/A:1010933404324

Campus, M., Degirmencioglu, N., Comunian, R., 2018. Technologies and trends to improve table olive quality and safety. Front. Microbiol. 9. https://doi.org/10.3389/fmicb.2018.00617

Cayuela, J.A., Camino, M. del C.P., 2010. Prediction of quality of intact olives by near infrared spectroscopy. Eur. J. Lipid Sci. Technol. 112, 1209–1217. https://doi.org/10.1002/ejlt.201000372

Chávez F.,. Vivas A, Moñino M. J. Fernández F., 2019. METSK-HD-Angeleno: How to predict fruit quality using Multiobjective Evolutionary learning of TSK systems. 2019 IEEE Congress on Evolutionary Computation (CEC), Wellington, New Zealand, 1251-1258. doi:10.1109/CEC.2019.8790268

Cubero, S., Aleixos, N., Albert, F., Torregrosa, A., Ortiz, C., García-Navarrete, O., Blasco, J., 2014. Optimised computer vision system for automatic pre-grading of citrus fruit in the field using a mobile platform. Precis. Agric. 15, 80–94. https://doi.org/10.1007/s11119-013-9324-7

Santosh Kumar Dash, M.P., 2016. Image Classification Using Data Mining Techniques. Adv. Comput. Sci. Inf. Technol. Volume 3, 157–162. https://doi.org/10.13140/RG.2.1.1064.7928

de Jódar Lázaro, M., Luna, A.M., Lucas Pascual, A., Martínez, J.M.M., Canales, A.R., Madueño Luna, J.M., Segovia, M.J., Sánchez, M.B., 2020. Deep learning in olive pitting machines by computer vision. Comput. Electron. Agric. 171, 105304. https://doi.org/10.1016/j.compag.2020.105304

Diaz, R., Faus, G., Blasco, M., Blasco, J., Moltó, E., 2000. The application of a fast algorithm for the classification of olives by machine vision. Food Res. Int. 33, 305–309. https://doi.org/10.1016/S0963-9969(00)00041-7

Diaz, R., Gil, L., Serrano, C., Blasco, M., Moltó, E., Blasco, J., 2004. Comparison of three algorithms in the classification of table olives by means of computer vision. J. Food Eng. 61, 101–107. https://doi.org/10.1016/S0260-8774(03)00191-2

Djurovic, I., 2017. Combination of the adaptive Kuwahara and BM3D filters for filtering mixed Gaussian and impulsive noise. Signal, Image Video Process. https://doi.org/10.1007/s11760-016-1019-x

Dumanay, A.B., Sakin, R., İstanbullu, A., 2016. A New Design of Olive Fruit Sorting Machine Using Color Image Processing.Org 9, 41–47. https://doi.org/10.9790/2380-0911014147

Ferreira, J. 1979. Explotaciones olivareras colaboradoras nº 5. Ministerio de Agricultura. Madrid.

Food and Agriculture Orgnization (FAO).2013. Codex standard for table olives. Available on http://www.fao.org/fao-who-codexalimentarius/codex-texts/list-standards/en/ (04/02/2020)

Furferi, R., Governi, L., Volpe, Y., 2010. ANN-based method for olive Ripening Index automatic prediction. J. Food Eng. 101, 318–328. https://doi.org/10.1016/j.jfoodeng.2010.07.016

Gatica, G., Best, S., Ceroni, J., Lefranc, G., 2013. Olive fruits recognition using neural networks. Procedia Comput. Sci. 17, 412–419. https://doi.org/10.1016/j.procs.2013.05.053

Guzman, E., Baeten, V., Pierna, J.A.F., García-Mesa, J.A., 2015. Determination of the olive maturity index of intact fruits using image analysis. J. Food Sci. Technol. 52, 1462–1470. https://doi.org/10.1007/s13197-013-1123-7

Haff, R.P., Saranwong, S., Thanapase, W., Janhiran, A., Kasemsumran, S., Kawano, S., 2013. Automatic image analysis and spot classification for detection of fruit fly infestation in hyperspectral images of mangoes. Postharvest Biol. Technol. 86, 23–28. https://doi.org/10.1016/j.postharvbio.2013.06.003

International Olive Council (IOC), 2018. Table olive figures. Available on https://www.internationaloliveoil.org/what-we-do/economic-affairs-promotion-unit/#figures (04/02/2020)

Jiménez, F. J., Castro-García, S., Blanco-Roldán, G. L., Sánchez, E. J. G., Gil-Ribes, J. A. , 2013. Isolation of table olive damage causes and bruise time evolution during fruit detachment with trunk shaker. Spanish journal of agricultural research, (1), 65-71. http://dx.doi.org/10.5424/sjar/2013111-3399

Kohno, Y., Kondo, N., Iida, M., Kurita, M., Shiigi, T., Ogawa, Y., Kaichi, T., Okamoto, S., 2011. Development of a mobile grading machine for citrus fruit. Eng. Agric. Environ. Food 4, 7–11. https://doi.org/10.1016/S1881-8366(11)80002-9

Li, B., Lecourt, J., Bishop, G., 2018. Advances in non-destructive early assessment of fruit ripeness towards defining optimal time of harvest and yield prediction—A review. Plants, 7(1), 3. https://doi.org/10.3390/plants7010003

Martínez, S. S., Gila, D. M., Beyaz, A., Ortega, J. G., García, J. G, 2018. A computer vision approach based on endocarp features for the identification of olive cultivars. Computers and Electronics in Agriculture, 154, 341-346. https://doi.org/10.3390/S18113826

Méndez, V., Pérez-Romero, A., Sola-Guirado, R., Miranda-Fuentes, A., Manzano-Agugliaro, F., Zapata-Sierra, A., Rodríguez-Lizana, A., 2019. In-field estimation of orange number and size by 3D laser scanning. Agronomy 9. https://doi.org/10.3390/agronomy9120885

Menesatti, P., Angelini, C., Pallottino, F., Antonucci, F., Aguzzi, J., Costa, C., 2012. RGBcolour calibration for quantitative image analysis: the ‘‘3D Thin-Plate Spline” warping approach. Sensors, 12, 7063–7079. http://dx.doi.org/10.3390/s120607063

Morales-Sillero, A., Rallo, P., Jiménez, M. R., Casanova, L., & Suárez, M. P., 2014. Suitability of two table olive cultivars (‘Manzanilla de Sevilla’and ‘Manzanilla Cacerena’) for mechanical harvesting in superhigh-density hedgerows. HortScience, 49(8), 1028-1033.https://doi.org/10.21273/HORTSCI.49.8.1028

Navarro Soto, J., Satorres Martínez, S., Martínez Gila, D., Gómez Ortega, J., Gámez García, 2018. Fast and reliable determination of virgin olive oil quality by fruit inspection using computer vision. Sensors, 18(11), 3826. https://doi.org/10.3390/S18113826

Omid, M., Khojastehnazhand, M., Tabatabaeefar, A., 2010. Estimating volume and mass of citrus fruits by image processing technique. J. Food Eng. 100, 315–321. https://doi.org/10.1016/j.jfoodeng.2010.04.015

Opara, U. L., Pathare, P. B., 2014. Bruise damage measurement and analysis of fresh horticultural produce—a review. Postharvest Biology and Technology, 91, 9-24. https://doi.org/10.1016/j.postharvbio.2013.12.009

Ortaç, G., Bilgi, A.S., Taşdemir, K., Kalkan, H., 2016. A hyperspectral imaging based control system for quality assessment of dried figs. Computers and Electronics in Agriculture, 130, 38-47. https://doi.org/10.1016/j.compag.2016.10.001

Ponce, J.M., Aquino, A., Millán, B., Andújar, J.M., 2018. Olive-fruit mass and size estimation using image analysis and feature modeling. Sensors (Switzerland) 18. https://doi.org/10.3390/s18092930

Riquelme, M.T., Barreiro, P., Ruiz-Altisent, M., Valero, C., 2008. Olive classification according to external damage using image analysis. J. Food Eng. 87, 371–379. https://doi.org/10.1016/j.jfoodeng.2007.12.018

Serranti S., Bonifazi G., Gasbarrone R.,2018.Olive fruit ripening evaluation and quality assessment by hyperspectral sensing devices., Proc. SPIE 10665, Sensing for Agriculture and Food Quality and Safety X, 106650R (15 May 2018). https://doi.org/10.1117/12.2297352

Sola-Guirado, R. R., Castillo-Ruiz, F. J., Blanco-Roldan, G. L., Gonzalez-Sánchez, E., Castro-García, S., 2020. Mechanical canopy and trunk shaking for the harvesting mechanization of table olive orchards. Revista de la Facultad de Ciencias Agrarias UNCuyo.

Srivastava, S., Sadistap, S., 2018. Non-destructive sensing methods for quality assessment of on-tree fruits: a review. J. Food Meas. Charact. 12, 497–526. https://doi.org/10.1007/s11694-017-9663-6

Tsouvaltzis, P., Babellahi, F., Amodio, M.L., Colelli, G., 2020. Early detection of eggplant fruit stored at chilling temperature using different non-destructive optical techniques and supervised classification algorithms. Postharvest Biology and Technology, 159, 111001. https://doi.org/10.1016/j.postharvbio.2019.111001

Tu, K.Y., 2009. Analysis of camera’s images influenced by varying light illumination for design of color segmentation. J. Inf. Sci. Eng. 25, 1885–1899. https://doi.org/10.6688/JISE.2009.25.6.14

Zhang, B., Gu, B., Tian, G., Zhou, J., Huang, J., Xiong, Y., 2018. Challenges and solutions of optical-based nondestructive quality inspection for robotic fruit and vegetable grading systems:

A technical review. Trends Food Sci. Technol. 81, 213–231.
https://doi.org/10.1016/j.tifs.2018.09.018